DYNAMIC PERFORMANCE OF A FORCED CONVECTIVE DIRECT STORAGE SYSTEM USING WATER AND PHASE CHANGE MATERIALS FOR LOW TEMPERATURE APPLICATIONS

Teamah H.M.[1], Lightstone M.F.[1], Cotton, J.S.[1]
[1]McMaster University, Hamilton, Ontario, Canada
teamahhm@mcmaster.ca , lightsm@mcmaster.ca, cottonjs@mcmaster.ca

ABSTRACT

The paper presents the heat transfer characteristics of a shell and tube latent thermal energy storage system. A two dimensional computational fluid dynamics model based on enthalpy porosity was developed to investigate the charging and discharging of the system. Organic fatty acids were used as phase change materials in the tubes and water was used as heat transfer fluid in the shell. A variety of numerical investigations were carried out for both constant and variable inlet temperature profiles. The gains in energy storage for the studied system were compared to a sensible water-only system. The melting times were found to be reasonable (less than 12 hours) and a gain in stored energy from 132-376% can be obtained by increasing phase change volume fraction from 30% to 80% for a 7 ^{o}C operating range of temperature.

NOMENCLATURE

A_{tank}	Outer surface Area of the tank [m^2]
C_{pl}	Liquid specific heat capacity [J/kg K]
C_{ps}	Solid specific heat capacity [J/kg K]
D_h	Hydraulic diameter [m]
E	Energy stored [J]
H	Dimensionless specific enthalpy
h	Heat transfer coefficient [W/m^{2}K]
i	Specific enthalpy [J/kg]
K	Thermal conductivity [W/mK]
L_c	Length of cylinder [m]
M	Number of axial nodes
$\dot{m}$	Mass flow rate inlet to the tank [kg/s]
N	Number of radial nodes
N_c	Number of cylinders in the tank
Nu_c	Nusselt number based on cylinder outer radius
T	Temperature [^{o}C]
$R_{c,inn}$	Inner radius of phase change material cylinder [m]
$R_{c,out}$	Outer radius of phase change material cylinder [m]
r_s	Latent heat [kJ/kg]
Re	Reynolds number

T_{st}	Initial (start) temperature of the tank [^{o}C]
$U_{f,mean}$	Mean fluid velocity [m/s]
V	Volume of control volume [m^3]
V_{tank}	Tank volume [m^3]
ΔF_o	Fourier number
Δt	Time step [seconds]
ΔT_m	Transition melting range [^{o}C]
Nu_p	Nusselt number based on Dittis Botter correlation

Abbreviations

CFD	Computational fluid dynamics
HTF	Heat transfer fluid
LES	Latent energy storage
PCM	Phase change material
SDHW	Solar domestic hot water
SES	Sensible energy storage
TES	Thermal energy storage

Latin symbols

ε	Convergence criteria
θ	Dimensionless temperature
μ	Dynamic viscosity
ρ	Density
Σ	Summation

Superscripts

it	Current iteration level
It-1	Previous iteration level

Subscripts

c,inn	Inner surface of cylinder
c,out	Outer surface of cylinder
conv	Convective
f	Fluid
f,m	Mean for fluid
In	Inlet
k	Inner surface of control volume
k-1	Outer surface of control volume
l	Liquid
m	Melting
m$_1$	Lower melting
m$_2$	Upper melting
st	Start
t	Transition
∞	Surrounding

INTRODUCTION

Building energy use in the residential sector currently accounts for 17% of Canada's secondary energy consumption, where secondary energy is defined as the total amount of energy consumed by an end-use, and excludes the energy consumed to convert the energy into a useable form from its primary resource [1]. The breakdown by end-use within the residential sector shows that water heating accounts for 17% of the secondary energy consumption, while space heating accounts for 63% (i.e. a total of 80% for both sectors). For those two end-uses in Canada, heating is mainly provided by either electricity or natural gas. Assuming 4% annual growth of energy consumption rate, it was found that the natural gas reserves would only last until 2070 [1]. Other relevant yet critical issues are the climate changes and the global warming problems associated with fossil fuel consumption. There is thus a need to find alternative renewable resources; one of them is making use of solar radiation to heat water directly and on-site. However, solar energy is characterized by its intermittent nature owing to the day-night cycle and different seasons of the year. In order for the solar energy to be effectively used to follow specific demand patterns; energy storage systems should be carefully designed to compensate for the mismatch between the times when the solar energy is available and the times when there is energy demand.

Besides solar applications, thermal energy storage plays a vital role in many other applications as well; such as space refrigeration and air-conditioning, agricultural processes. And, in addition to space, automotive and waste heat recovery applications. Waste heat recovery has great potential in industrialized countries and depending on the temperature at which the waste heat is discharged it can be classified into three categories: (1) Low temperature waste heat (below 100 °C), (2) High temperature waste heat (above 400 °C) and (3) Moderate temperature waste heat (between 100 °C and 400 °C) [1]. Our interest throughout this study lies in the low temperature waste heat category which fits into the hot water and space heating applications of residential and commercial sectors. Most of the thermal energy storage applications have been studied and summarized in reviewed articles by Zalba et al. [2], Sharma et al [3], and Abhat [4].

There are three types of TES systems: (1) Sensible energy, (2) Latent energy and (3) Thermo-chemical storage (TCS) systems. Latent energy storage (LES) systems employ phase change materials (PCMs) and the energy is stored and released in the form of latent heat of fusion. LES systems have recently captured more attention in various applications owing to their high energy storage density compared to SES systems and their ability to store energy at constant temperature corresponding to the melting temperature (T_m) of the PCM used. The challenge is that, most PCMs are characterized by low thermal conductivity, low specific heat capacity and high cost. Common examples of PCMs used in LES systems are: paraffin, fatty acids, organic eutectics and hydrated salts. In order to determine an appropriate PCM for an application, a number of factors must be considered. Phase change temperature of a desirable PCM must be within the operating temperature range of the thermal storage system. Ideally, the specific heat of a PCM should be high when it is storing heat as sensible, and the thermal conductivity of the PCM should be high to ensure high heat transfer rates from the surface to the core of the PCM module in the system.

Abhat [4] classified PCMs into three categories: organic, inorganic and eutectics. Sharma et al. [3] extended Abhat's division with subcategories classifying the organic into paraffin and non-paraffin compounds, the inorganic into salt hydrate and metallic and finally eutectics into (organic-organic), (inorganic-inorganic) and (inorganic-organic). Paraffin waxes are a family of straight chain alkanes. Their melting temperature and latent heat increase with the hydrocarbon chain length [5-6], they are generally chemically stable, melt congruently and are non-toxic. However, paraffin wax has several disadvantages which are: moderate flammability and low thermal conductivity which limits its wide application in industry (Lane [7]). Non-paraffin organic PCMs consist of fatty acids, esters, alcohols and glycols; among them, fatty acids are promising for applications in solar thermal systems [8-10]. The most commonly used fatty acids are divided into six groups: caprylic, capric, lauric, myristic, palmitic and stearic with respectively 8 to 18 carbon atoms per molecule. Their melting points are in the range from 16°C to 65°C with a heat of fusion between 155 and 180 kJ/kg which is higher than paraffin waxes [11]. Thermal and physical properties of lauric acid were investigated by Desgrosseillier et al. [12]; results proved that lauric acid is a promising candidate for LES [13-15].

The main problem associated with the PCMs operating in low temperature is their low thermal conductivity which ranges from 0.1-0.6 [W/m.K]. This can limit the storage capacity for LES systems for a given charging or discharging time. Extensive research has been carried out to investigate heat transfer enhancements in latent heat thermal storage systems. The enhancement techniques can be classified into active and passive heat augmentation techniques [16-17], Active techniques include the application of an external source such as electro-hydrodynamics to enhance the melting rate as studied by Nakhla et al. [16]. Passive techniques can be mainly divided into different categories [18-19]: using extended surfaces, thermal conductivity enhancement, micro-encapsulation of PCM and Using multiple PCMs.

Extended surface techniques such as fins are based on increasing the heat transfer area in the thermal system to increase the total rate of heat transfer. Fins offer an increased area advantage, while they have an adverse effect on the weight, the volume and cost of the thermal storage system for a given storage energy required [16-19]. Also, some research used metallic particles to enhance the thermal conductivity and limit the charging and discharging times to be within acceptable limits but the main disadvantage of this technique is being intrusive in nature and the thermo-physical properties of PCMs are altered [20-22]. Trying to reduce the PCM thermal resistance by encapsulating it in thin modules and geometric optimization was a third aspect of enhancement techniques [23-25].

Using multiple PCMs captured the attention of researchers for concentrated solar power applications. Michels and Pitz-Paal [26] experimentally tested on the cascaded latent heat storage system for parabolic trough solar power plants in which three different PCMs were used. The experiments were conducted to investigate the effect of employing LES systems using PCMs with different melting temperatures arranged in series. High temperature oil was used as the heat transfer fluid with charging temperature of 390 °C and discharging temperature at 285 °C. They concluded that cascaded LES systems with multiple PCMs provide high storage potentials compared to the sensible system if the PCM thermal conductivity is increased by 4 times. This highlights the limitation of the low thermal conductivity of PCMs. Also, they showed that the energy storage in the cascaded

system is higher than using only one of the PCMs (around 74%). Seeniraj and Narasimhan [27] used fins to enhance heat transfer in a multi-PCM thermal storage system. They found that the molten fraction increased by 35% in comparison to a single PCM model.

Recent research studied the hybrid energy storage to take the advantages of both sensible and latent storages, Nallusamy et al. [28] investigated experimentally the thermal behavior of a packed bed TES system that consisted of spherical PCM capsules (paraffin with $T_m = 60$ °C) surrounded by SES medium (water). Their results showed that employing PCM in the TES system leads to better control of the HTF flow temperature owing to the constant melting temperature of the PCM. However, the first layer of the spherical capsules receiving the HTF flow showed faster melting rate than the last layer further downstream. This led to more energy stored in the liquid PCM in the form of sensible energy which is at least one order of magnitude less than the latent heat of fusion of the same PCM at the same temperature operation range of the experiments.

The heat transfer mechanism in a cylindrical tube heat exchanger with PCM was studied by Shmueli et al., [29]. Numerical results showed that at the beginning of the process, heat was transferred by conduction from the tube wall to the solid phase PCM through a relatively thin liquid layer. As the melting progressed, natural convection in the liquid became the dominant heat transfer mode. Jones et al. [30] performed an experimental and numerical study exploring the thermal characteristics of melting n-eicosane as the PCM in a cylinder with constant wall temperature boundary condition. They captured the melt front at different stages; it was dominated by conduction in the early stages and eventually convection dominated and they recommended one of their conducted experiments for numerical benchmarking.

Predicting the thermal behaviour of phase change materials is difficult because of the inherent non-linear nature at moving interfaces. Three sets of numerical methods for solving for heat transfer in latent heat energy storage systems were summarized by Dutil et al. [31]: namely fixed grid; adaptive mesh; and first law and second law of thermodynamics methods. Because of their conceptual simplicity, fixed grid approaches have found a wide application. The essential feature of fixed grid approaches is that the latent heat evolution is accounted for in the governing

equations by defining either an enthalpy, or an effective specific heat, or a heat source (or sink). Consequently, the numerical solution can be carried out on a space grid that remains fixed throughout the calculation process.

The major problem with fixed grids enthalpy methods is in accounting for the zero velocity condition as the liquid region turns to solid. Morgan [32] employed the simple approach of fixing the velocities to zero in a computational cell whenever the mean latent heat content, reaches some predetermined value between 0 (cell all solid) and L (cell all liquid), where L is the latent heat of the phase change. Voller et al. [33-35] have investigated various ways of dealing with the zero solid velocities in fixed grid enthalpy solutions. Computational cells in which phase change is occurring are modelled as pseudo porous media with the porosity, decreasing from 1 to 0 as latent heat content of the cell decreases from latent heat of fusion value to zero.

The other widely used fixed grid method is the "heat capacity method". With this method the latent heat effect is approximated by a large effective heat capacity over a small temperature range [36-40]. This approach is simple in concept and easy to implement. It is, however, sensitive to the choice of the phase change temperature interval and the integration scheme and in some cases the correct solution or even a solution cannot be obtained due to non-convergence caused by the sudden change of the specific heat at the interface.

The present work employs the enthalpy porosity method due to its recommended simplicity and stability over wide temperature ranges in different applications

A study of the literature has shown that careful design of TES systems is very critical to obtain enhanced utilization of renewable sources as well as to the efficient recovery of waste heat. This will in turn lead to significant reduction in the system's size in addition to a reduction of greenhouse gas (GHG) emissions. Employing both SES and LES was not well explored in the available literature. This motivated the current research work to study the performance of a hybrid storage system that uses water and organic PCMs to harvest the advantages and minimize the disadvantages of both media.

NUMERICAL MODELLING

An enthalpy porosity model is developed to deal with phase change process which takes into account the following assumptions:
1) PCM is homogenous and isotropic
2) Thermo-physical properties of PCM are different for different phases but they are independent of temperature
3) The expansion of the PCM is neglected.

According to the enthalpy porosity formulation [41] specific enthalpy (enthalpy per unit mass) is defined based on the cell condition (solid, liquid or transition) as follows:

$$i(T) = C_{p,s}T \qquad\qquad T < T_{m1} \qquad (1)$$

$$i(T) = C_{p,s}T_{m1} + \frac{r_s(T - T_{m1})}{\Delta T_m} \qquad (2)$$

$$T_{m1} < T < T_{m2}$$

$$i(T) = C_{p,l}(T - T_{m2}) + r_s + C_{p,s}T_{m1} \qquad (3)$$

$$T > T_{m2}$$

r_s is the latent heat, T_{m1} is the lower melting temperature and T_{m2} is the upper melting temperature.

By introducing the following non-dimensional expressions for enthalpy and temperature;

$$H = \frac{i - i_{m1}}{r_s} \qquad (4)$$

$$\theta = \frac{C_{p,s}(T - T_{m1})}{r_s} \qquad\qquad T < T_{m1} \qquad (5)$$

$$\theta = \frac{C_{p,l}(T - T_{m1})}{r_s} \qquad\qquad T > T_{m1} \qquad (6)$$

By using expressions [4-6] together with the finite differencing in the conduction dominated melting equation and considering the geometry of element shown in figure 1; it yields;

$$H_{j,k}^i - H_{j,k}^{i-1}$$
$$= \Delta F_o[a_k(\theta_{j,k+1}^i - \theta_{j,k}^i) + b_k(\theta_{j,k-1}^i - \theta_{j,k}^i)$$
$$+ C_1(\theta_{j+1,k}^i - \theta_{j,k}^i)$$
$$+ C_2(\theta_{j-1,k}^i - \theta_{j,k}^i)] \qquad (7)$$

Where;

$$\Delta F_o = \frac{k_{j,k}\Delta t}{\rho C_{p,j,k} R_{c,out}^2} \qquad (8)$$

$$a_k = \frac{4 r_k}{(r_{k-1} - r_{k+1})(r_{k-1}^2 - r_k^2)} \qquad (9)$$

$$b_k = \frac{4 r_{k-1}}{(r_{k-2} - r_k)(r_{k-1}^2 - r_k^2)} \qquad (10)$$

$$C_1 = C_2 = \frac{R_{c,out}^2}{L^2} \qquad (11)$$

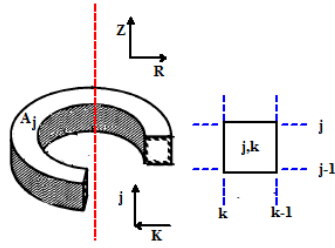$$r_k = \frac{R_k}{R_{c,out}} \qquad (12)$$

Figure 1 studied element geometry

The code was validated on a 2D problem for melting with constant wall temperature condition presented by Jones et al. [30]. The schematic of their test facility is shown in figure 2, an isothermal boundary condition was maintained by immersing the n-eicosane cylinder in a water bath. The present results were compared to both their experimental and numerical predictions as shown in figure 3, which indicated a very good agreement with both the experimental and numerical molten fractions.
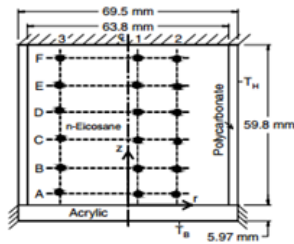
Figure 2: Schematic of the experimental facility by Jones et al [30]
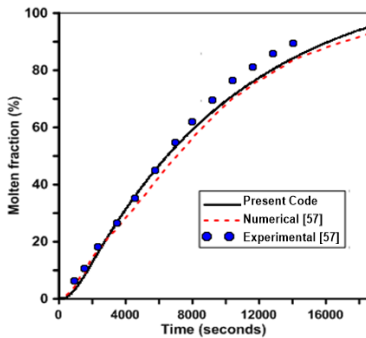
Figure 3: Comparison of present code and Jones et al. [30].

The code was also accommodated to deal with rectangular co-ordinates. From the literature, the most commonly used PCM encapsulations are rectangular and cylindrical. The following subsection presents a comparison between their performance.

Comparison of cylindrical and rectangular performance

The storage tank considered in the present study is a part of domestic heating system. The Phase change materials are enclosed in thin modules to minimize thermal resistance imposed by the low thermal conductivity of the PCM. Preliminary simulations were conducted to compare the performance of rectangular module and equivalent array of cylindrical modules shown in figure 4 and 5.
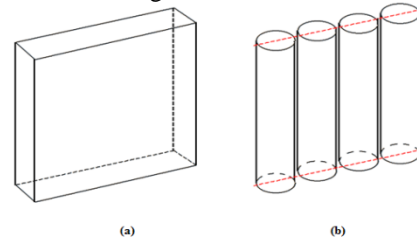

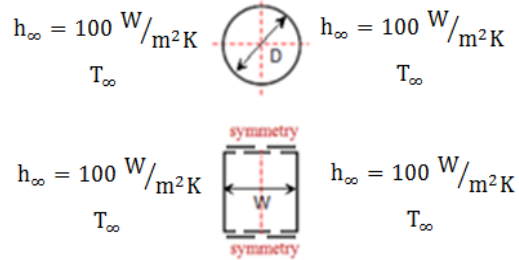Figure 4: (a) rectangular module and (b) equivalent cylinderical modules array

Figure 5: Boundary conditions for the studied modules

When considering the same volume for rectangular and cylindrical modules; i.e. the comparison between (100cm x 100cm x 2cm) rectangular slab with a 40 cylinder array; each of 2.25 cm diamter and 100 cm length initially at the melt temperature $T_m = 42°C$, the molten fraction (molten volume/total volume) is shown in figure 6. The melt propogates faster in the cylinderical modules, especially at the early stages of melting, then it relatively decreases owing to the decreased heat transfer area when melt progresses but the overall performance of the cylinderical module is better. Also, Figure 7 shows that the ratio between the actual molten fraction and the ideal molten fraction is higher for the cylindrical module compared to the rectangular one (Ideal denotes the case where the PCM conductivity is infinite so all the convective heat transfer is utilized in the melting process without considering the liquid PCM superheating; the ideal melting time is computed as $t_{melt,ideal} = \frac{mass*r_s}{h_\infty A(T_\infty - T_m)})$
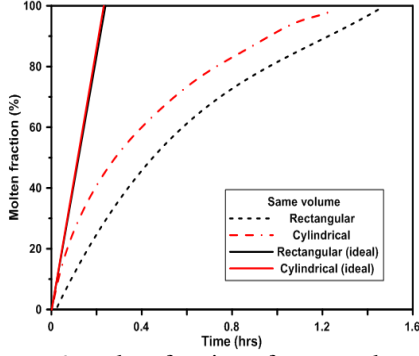
Figure 6: molten fraction of rectangular and cylindrical modules versus time considering same volume ($h_\infty = 100 \ ^W/_{m^2K}$, $T_\infty = 52 \ ^\circ C$)
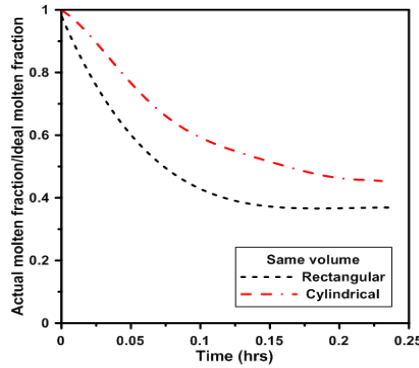

Figure 7: Ratio of actual molten fraction to ideal molten fraction for cylindrical and rectangular modules versus time considering same volume ($h_\infty = 100 \ ^W/_{m^2K}$, $T_\infty = 52 \ ^\circ C$)

By keeping the same conduction distance for both rectangular and cylindrical modules (i.e 2 cm diameter cylindrical modules and 2 cm thick rectangular one), and by maintaining the same heat transfer area and the volume to area ratio, the same trend is also observed. This result agrees with Barba and Spiga [24], who proved analytically that the retrieval rate of energy is higher in the cylindrical module than that of the rectangular one. The difference between the present work and their work is the different operating temperature ranges and properties of the used PCMs.

Based on the previous results, cylindrical modules seem to perform better than rectangular ones; so the tank considered in the present work consists of cylindrical pipes containing phase change material surrounded by water flowing parallel to it as shown in figure 8. During the charging process hot water is introduced to the top of the tank and in discharging

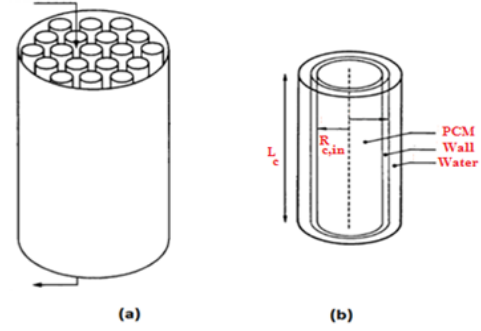the extracted hot water to meet the load is compensated with cold water from the mains.

Figure 8: the studied domain in the code (a) the whole tank, (b) the cylindrical jacket

The developed enthalpy porosity model is expanded to take into account the heat transfer from the water surrounding the PCM cylinders by using the correlations presented by Rhosenow [42] where;

For laminar flow

$$Nu_c = 3.66 + 4.12 \left(^{D_h}/_{R_{c,out}} - 0.205\right)^{0.569} \qquad (13)$$

$$if \quad Re_c \le 2200$$

For turbulent flow

$$\frac{Nu_c}{Nu_p} = 1.08 - 0.794 \ e^{-1.62 \ D_h/_{R_{c,out}}} \qquad (14)$$

$$if \ Re_c \ge 2200$$

Where;

$$Re_c = \frac{\rho_f U_{f,mean} D_h}{\mu_f} \qquad (15)$$

$$D_{h,c} = \frac{2}{\pi} \frac{V_{tank}}{N_c R_{c,out} L_c} - 2R_{c,out} \qquad (16)$$

The mean velocity can be calculated as follows (assuming uniform flow distribution);

$$U_{f,m} = \frac{\dot{m}}{\rho_f \left(^{V_{tank}}/_{L_c} - \pi N_c R_{c,out}^2\right)} \qquad (17)$$

Applying energy balance on the HTF, wall and PCM control volumes yields a system of equations; this set can be solved with Gauss-Seidl iterative method. At specific time level i the entire field is defined by H and θ for the phase change material and T values for the wall and the heat transfer fluid. After another time step the new values of H, θ and T are calculated. Then a convergence test is done. Dependent on the result of that test, iteration is executed at the same time level or

the time level is increased. This convergence criteria is given by;

$$\left| \frac{T_{j,k}^{i,it} - T_{j,k}^{i,it-1}}{T_{j,k}^{i,it} + T_{j,k}^{i,it-1}} \right| < \varepsilon \tag{18}$$

ε is a specified convergence criterion based on the desired accuracy level

RESULTS AND DISCUSSION

A commercial 200 L tank is considered in the present study with length 78 cm. The number of the PCM cylinders varies according to the packing ratio (PCM volume/ total volume). Dimensions and studied parameters are summarized in Table 1. Thermo-physical properties of the utilized fatty acids are listed in table 2.

Table 1: Dimensions and studied parameters

Tank volume	200 litres (0.2 m^3)
Tank length	78 cm
Tank diameter	57 cm
PCM module diameter	2 cm, 4 cm and 8 cm
PCM packing ratio	30%, 50% and 80%
Mass flowrate	$\dot{m} = 0.05 - 0.5$ Kg/s

Table 2: Thermo-physical properties of organic fatty acids [4]

Acid	T_m [℃]	C_p [kJ/kg K]	r_s [kJ/kg]	K_s W/m. k
Capric	31.5	NA*	153	0.149
Lauric	42	1.6	178	0.147
Myristic	54	1.6(solid), 2.7(liquid)	187	NA*
Palmitic	63	NA*	187	0.165

*Not available in the literature

At first simulations were done to test the charging process of the tank with its initial temperature 40° C. The inlet water to the tank has a mass flow rate of 0.05 kg/s and temperature of 52°C. Lauric acid is used as the PCM (T$_m$= 42 ^{o}C) and it is placed in 2 cm diameter cylinders.

Figure 9 shows the grid independence test where a grid of 300 nodes in the radial direction and 100 nodes in the axial direction together with 0.005 time step will be the most computationally efficient one to solve the problem. It is also shown that it takes 3.2 hours to melt the PCM in the 30% packing ratio condition.
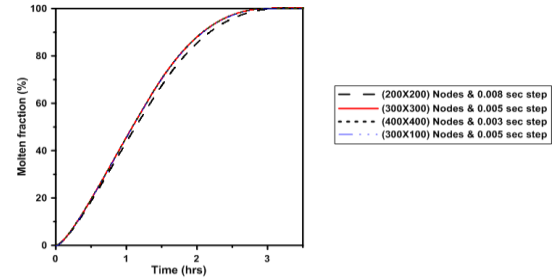

Figure 9: Grid independence test for molten fraction result ($V_{tank} = 0.2$ m^3, packing ratio = 30%, $T_{st} = 40$ ℃, $T_{in} = 52$ ℃, $\dot{m} = 0.05$ kg/s)

The change in the stored energy with time in the PCM and HTF is shown in figure 10. After fully melting the PCM, 16.4 MJ of energy will be stored in the tank 61.8 % of it is stored in the PCM and 38.2% is stored in water. This corresponds to 65% gain in energy compared to the only water system

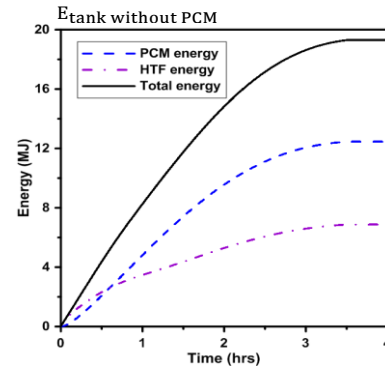$$gain = \frac{E_{tank\ with\ PCM} - E_{tank\ without\ PCM}}{E_{tank\ without\ PCM}}$$

Figure 10: evolution of energy with time in the system components ($V_{tank} = 0.2$ m^3, packing ratio = 30%, $T_{st} = 40$ ℃, $T_{in} = 52$ ℃, $\dot{m} = 0.05$ kg/s

Examining figure 11, which shows the isothermals during melting 30% PCM (T$_m$ = 42 ℃) in charging the tank (T$_{st}$ = 40 ℃, T$_{in}$ = 52 ℃, $\dot{m}$ = 0.05 kg/s) , it is clear that there is an axial variation in temperature in different levels of PCM module as water loses its energy axially throughout the way, which is also manifested in melt interface in figure 12. The higher levels of PCM modules melt and superheat before the lower levels.

Figure 13 shows the evolution of water temperatures at different heights of the tank (measured from tank top) the temperatures increase sensibly then it is tuned around the PCM melting temperature (due to the effect of PCM internal resistance) and then it superheats. Due to the axial variation of HTF temperature it shows both temporal and spatial variations.
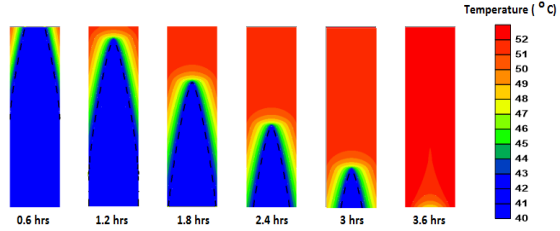
Figure 11: Isothermals in PCM modules in a 200 litre tank with 30 % PCM ($T_{st} = 40$ °C, $T_{in} = 52$ °C, $T_m = 42$ °C, $\dot{m} = 0.05$ kg/s) [melting point is shown in dotted line]
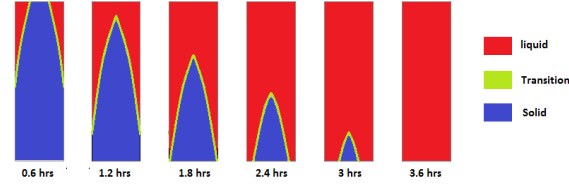
Figure 12: Isothermals in PCM modules in a 200 litre tank with 30 % PCM ($T_{st} = 40$ °C, $T_{in} = 52$ °C, $T_m = 42$ °C, $\dot{m} = 0.05$ kg/s) [melting point is shown in dotted line]
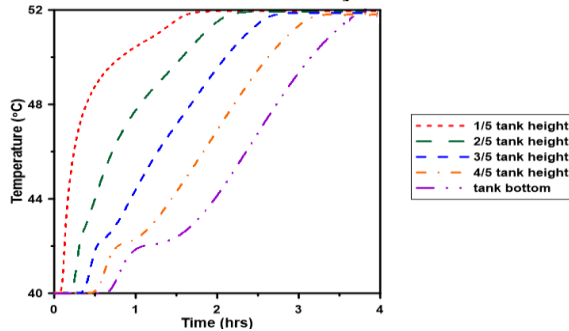
Figure 13: Temperature evolution in a 200 litre tank with 30 % PCM
($T_{st} = 40$ °C, $T_{in} = 52$ °C, $T_{in} = 42$ °C, m = 0.05 kg/s)

Narrowing the operating temperature range increases the gain from the system as the effect of latent heat of fusion will be more pronounced. For example, considering the inlet temperature to the tank to be 47°C instead of 52°C, the melting time becomes 6.2 hours instead of the 3.2 hours in the previous case. A total of 13.5 MJ is stored in the whole tank after fully melting the PCM, 72.4 % of the energy is stored in PCM and the rest in the HTF as shown in figure 14 and this makes the gain rise to 132% compared to the system without PCM. Also the PCM stores an increased percentage of the total energy 72.4% compared to 61.7% in the previous case (12°C operating temperature range). Table 3 summarizes the results for higher PCM packing ratios. As seen in

the table, the gain can reach as high as 362% compared to the SES using 80% PCM packing ratio and 7°C operating temperature range.
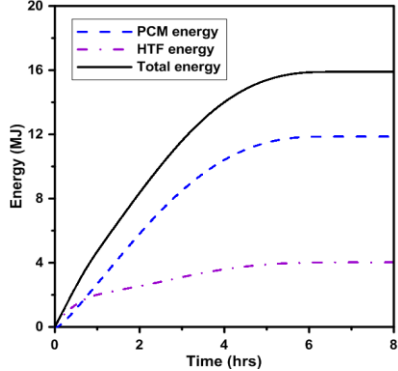

Figure 14: Energy evolution with time in a 200 litre tank with 30% PCM ($T_{st} = 40$ °C, $T_{in} = 47$ °C , $\dot{m}$= 0.05 kg/s)

Table 3: Summary of simulation results

7 °C Operating range				
% PCM	PCM energy (MJ)	HTF energy (MJ)	Gain (%)	Melting time (hrs)
30	9.82	3.78	132	6.1
50	16.22	2.37	218	8.3
80	25.9	1.1	362	10.4

To assess the impact of the non-ideal properties of the PCM, the results can be compared to the maximum analytical gain. The analytical gain is computed when all the system temperature becomes equal to the inlet fluid temperature which is the ultimate case achieved after giving the system an infinite time to charge.

$$\text{Analytical gain} = \frac{\text{Maximum energy stored in hybrid system}}{\text{Energy of tank without PCM}}$$

Figure 15 shows the analytical gain for different operating temperature ranges depending on the packing ratios. The gains that are expected from the simulation are less than those calculated analytically because by the end of PCM melting the whole tank would not be at the same inlet temperature and there would be an axial temperature variation across the HTF control volumes.
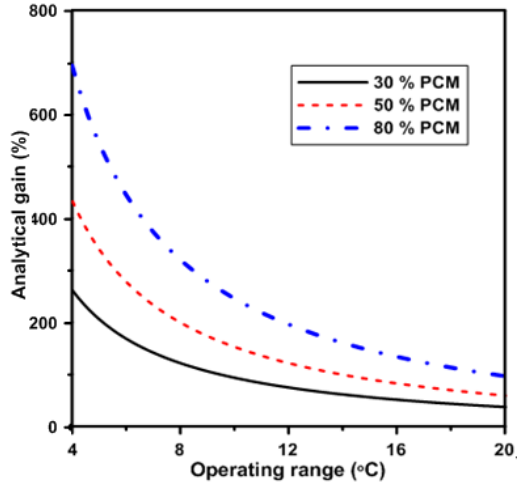
Figure 15: Analytical gains for different PCM ratios and range of temperature

The effect of varying mass flow rate on melting time for the case of 30% PCM packing ratio and 7°C operating range is shown in figure 16. The behaviour of HTF correlations is nonlinear so doubling the mass flow rate decreases the melting time significantly. Doubling the mass flow rate from 0.05 kg/s to 0.1 kg/s decreases the melting time to 69%. Increasing the flow rate 10 times reduces the melting time to 41%. This is due to the nonlinear behaviour of the heat transfer coefficient correlations. The melting time decreases to 38% with the very high mass flow rate as it will ensure a nearly constant temperature boundary condition on the PCM modules.
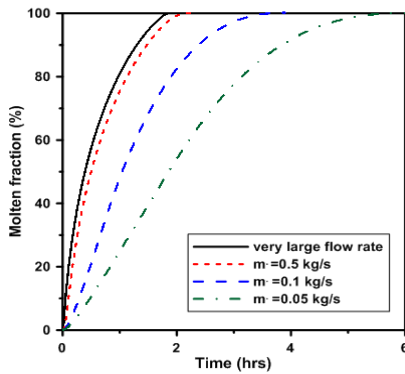

Figure 16: Effect of mass flow rate on melting time of 30% PCM ($T_{st} = 40\,^{\circ}$C, $T_{in} = 47\,^{\circ}$C)

Sequential charging and Discharging

Studying sequential charging and discharging is important in SDHW systems to see how the demand of typical families affects it. Figure 17 shows the temperature histories in a tank which is initially at

40 $^{\circ}$C when subjected to hot water from the top ($T_{in} = 60\,^{\circ}$C, $\dot{m} = 0.05\,\frac{kg}{s}$ and $T_m = 54\,^{\circ}$C) for 5 hours followed by discharging by cold water from the bottom ($T_{in} = 30\,^{\circ}$C, $\dot{m} = 0.1\,$kg/s) for 2 hours. It shows the tuning of temperature around the PCM temperature during both melting and solidification. Also, the higher levels of the tank are the first to be affected by the incoming hot charging water and the last to sense the cold discharging water.
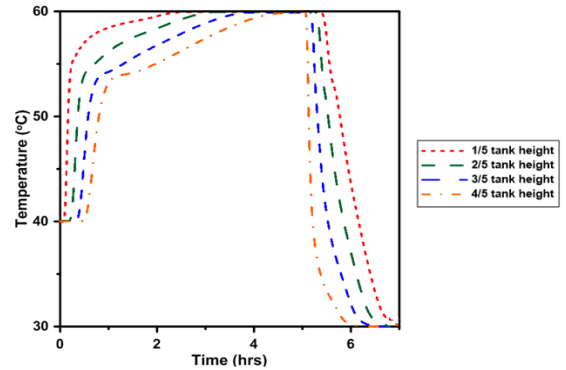

Figure 17: Temperature histories at different levels of 200 litres tank with 30 % PCM ($T_m = 53.8\,^{\circ}$C) under sequential charging and discharging

Variable charging profiles

To use the developed model for domestic applications, it should respond to the variable solar profiles. Figure 18 shows the effect of putting PCM with different packing ratios on temperature profiles in a 200 litres tank when subjected to a hypothetical sunny day profile. The temperatures are tuned during PCM melting and putting more percentage of the PCM evens out the peaks of outlet temperature relative to the case of no PCM where the tank obeys the plug flow model and the sine wave is only lagged by the tank turnover time.
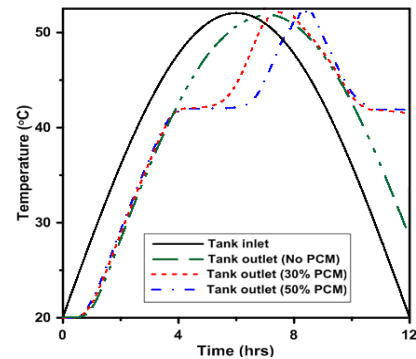

Figure 18: Temperature profiles in a 200 litres tank when subjected to a hypothetical sunny day profile ($T_m = 42\,^{\circ}$C, $\dot{m} = 0.05\,$kg/s)

Effect of PCM module diameter

Figure 19 shows contours of the predicted molten fraction and gains for a tank having 50% PCM under combinations of operating temperature ranges and charging periods it shows that increasing the PCM module diameter from 2 cm to 8 cm has a great effect on limiting the regions of high expected gains and also the predicted molten fractions are low compared to the smaller diameter due to less heat transfer area. Also negative gains can be obtained with the very low charging period that don't allow for the whole melting of the PCM and this can be attributed to the poor sensible properties of PCM compared to water.
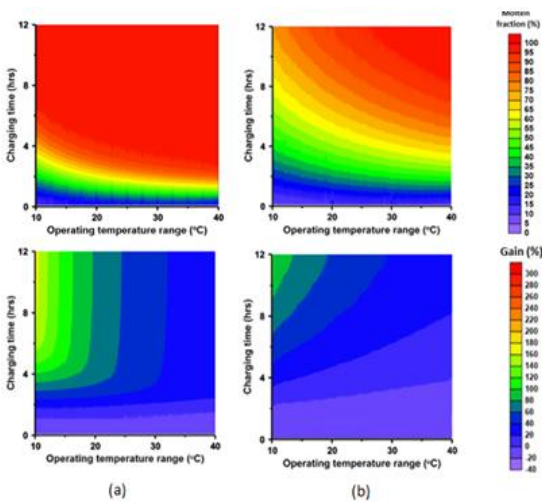

Figure 19: Melt fraction and gains for 50% PCM in a 200 liter tank ($T_{st} = 20°C$, $T_m = \frac{T_{st}+T_{in}}{2}$, $\Delta T_{op} = T_{in} - T_{st}$)

(a) 2 cm diameter module,
(b) 8 cm diameter module

CONCLUSION

A parametric study is conducted on hybrid tank used for residential application. Including PCM with packing ratios from 30% to 80% PCM increases the gains of the system 1.4-3.7 times compared to the only water system for $7°C$ operating range. The gains are very sensitive to the module diameter; smaller diameters increase the expected gains because of the higher heat transfer area. Higher mass flowrates reduce the melting times because of the higher heat transfer coefficient. Including PCM in a tank modulates the tank outlet temperature around its melting point. Care should be taken in choosing the correct PCM in different applications as when the charging period of the system is less than the required time to fully melt the PCM the incorporation

of PCM can yield negative gain compared to the only sensible system.

REFERENCES

[1] NRCan. "Energy Use Data Handbook - 1990 to 2009." Technical report, Office of Energy Efficiency, Natural Resources Canada, Ottawa, ON, Canada. [Online] http://oee.nrcan.gc.ca/Publications/statistics /handbook11/ (2012).

[2] Zalba, B., Marin, J. M., Cabeza, L. F., and Mehling, H. (2003), 'Review on thermal energy storage with phase change: materials, heat transfer analysis and applications', *Applied Thermal Engineering*, 23(3), 251-283.

[3] Sharma, A., Tyagi, V.V., Chen, C.R., and Buddhi, D. (2009), 'Review on thermal energy storage with phase change materials and applications', *Renewable and Sustainable Energy Reviews*, 13(2), 318-345.

[4] Abhat, A. (1983), 'Low temperature latent heat thermal energy storage: Heat storage materials', *Solar Energy*, 30(4), 313-332.

[5] Zhang Z.G. and Fang X.M. (2006), 'Study on paraffin/expanded graphite composite phase change thermal energy storage material', *Energy Conversion and Management*, 47, 303-310.

[6] Kousksou T., Jamil A., Eirhafiki T. and Zeraouli Y. (2010),'Paraffin wax mixtures as phase change materials', *Solar Energy Materials and Solar Cells*, 94, 2158-2165.

[7] Lane G. A. (1983),'*Solar heat storage: latent heat materials*', vol. I. Boca Raton, FL: CRC Press, Inc.

[8] Feldman D., Banu D., and Hawes D. (1995),' Low chain esters of stearic acid as phase change materials for thermal energy storage in buildings', *Solar Energy Materials and Solar Cells*, 36, 311-322.

[9] Feldman D., Banu D., and Hawes D. (1995), 'Development and application of organic phase change mixtures in thermal storage gypsum wallboard', *Solar Energy Materials and Solar Cells*, 36, 147-157.

[10] Alkan C. and Sari A. (2008), 'Fatty acid/poly (methyl methacrylate) (PMMA) blends as form-stable phase change materials for latent heat thermal energy storage', *Solar Energy*, 82, 118-124.

[11] Baetens R., Jelle B. and Gustavsen A. (2010),'Phase change materials for building applications: A state-of-the-art review', *Energy and Buildings*, 42, 1361-1368.

[12] Desgrosseillier L., Murray R., Safatli A., Marin G., Stewart J., Osbourne N., White M.A., Groulx D. (2011), 'Phase Change Material Selection in the Design of a Latent Heat Energy Storage System Coupled with a Domestic Hot Water Solar Thermal System', *ASHRAE Annual Conference*, Montreal, Canada.

[13] Sari A. and Kaygusuz K. (2002), 'Thermal and heat transfer characteristics in a latent heat storage system using lauric acid', *Energy Conversion and Management*, 43, 2493-2507.

[14] Sari A. and Kaygusuz K. (2003), 'Some fatty acids used for latent heat storage: thermal stability and corrosion of metals with respect to thermal cycling', *Renewable Energy*, 28, 939-948.

[15] Sari A. and Karaipekli A.(2009), 'Preparation, thermal properties and thermal reliability of palmitic acid/expanded graphite composite as PCM for thermal storage', *Solar Energy Materials and Solar Cells*, 93, 571-576.

[16] Nakhla D., Sadek H and Cotton J. S. (2015),'Melting performance enhancement in latent heat storage module using solid extraction electrohydrodynamics (EHD) ' *International Journal of Heat and Mass Transfer*, 81, 695-704.

[17] A. E. Bergles (2011), 'Recent developments in enhanced heat transfer', *Heat and mass transfer*, 47(8) , 1001-1008.

[18] S. Jegadheeswaran and S. D. Pohekar (2009), 'Performance enhancement in latent heat thermal storage system: A review', *Renewable and Sustainable Energy Reviews*, 13(9), 2225–2244.

[19] F. Agyenim, N. Hewitt, P. Eames and M. Smyth (2010), 'A review of materials, heat transfer and phase change problem formulation for latent heat thermal energy storage systems (LHTESS)' , *Renewable and Sustainable Energy Reviews*, 14(2), 615–628.

[20] O. Sanusi, R. Warzoha and A. S. Fleischer (2011), 'Energy storage and solidification of paraffin phase change material embedded with graphite nano-fibers', *International Journal of Heat and Mass Transfer*, 54(19), 4429–4436.

[23] U. Stritih (2004), 'An experimental study of enhanced heat transfer in rectangular PCM thermal storage', *International Journal of Heat and Mass Transfer,* 47(12-13), 2841–2847.

[24] Barba A., Spiga M. (2003), 'Discharge Mode for Encapsulated PCM's in Storage Tanks', *Solar Energy*, 32, 141-148.

[25] M. Lacroix and M. Benmadda, (1997) , 'Numerical Simulation of Natural Convection-Dominated Melting and Solidification From a Finned Vertical Wall', *Numerical Heat Transfer*, Part A: Applications, 31(1), 71-86.

[26] Michels, H., Pitz-Paal, R. (2007), 'Cascaded latent heat storage for parabolic trough solar power plants', *Solar Energy*, 81(6), 829-837.

[27] Seeniraj, R.V., Narasimhan, N.L. (2008), 'Performance enhancement of a solar dynamic LHTS module having both fins and multiple PCMs', *Solar Energy*, 82(6), 535-542.

[28] Nallusamy, N., Sampath, S., Velraj, R. (2007), 'Experimental investigation on a combined sensible and latent heat storage system integrated with constant/varying (solar) heat sources', *Renewable Energy*, 32, 7, 1206-1227.

[29] Shmueli H., Ziskind G. and Letan R. (2010), 'Melting in a vertical cylindrical tube: Numerical investigation and comparison with experiments', *International Journal of Heat and Mass Transfer*, 53, 4082-4091.

[30] Benjamin J. Jones, Dawei Sun, Shankar Krishnan, Suresh V. Garimella (2006) , 'Experimental and numerical study of melting in a cylinder", *International Journal of Heat and Mass Transfer*, 49 , 2724–2738.

[31] Dutil Y., Rousse D.R., Salah N.B., Lassue S., and Zalewski L. (2011),'A review on phase-change materials: Mathematical modeling and simulations', *Renewable and Sustainable Energy Reviews*, 15, 112-130.

[32] K. Morgan (1981) , 'A numerical analysis of freezing and melting with convection'. *Computational methods in applied engineering*, 28, 275-284.

[33] V. R. Volier. N. C. Markatos and M. Crass, (1985)' Techniques for accounting for the moving interface in convection/diffusion phase change'. *Numerical Methods in Thermal Problems*,4,595-609.

[34] V. R. Voller, N. C. Markatos and M. Cross (1986), 'Solidification in convection and diffusion', *Numerical Simulations of Fluid Flow and Heat/Mass Transfer Processes*, 24, 425-432.

[35] V. R. Voller, M. Cross and N. C. Markatos (1987), 'An enthalpy method for convection/diffusion phase changes'. *International Journal of Numerical Methods in Engineering*, 24, 271-284.

[36] Bonacina, C., Cornini, G., Fasano, A and Primicero, M. (1973), 'Numerical Solution of Phase-Change Problems', *Int. Journal of Heat and Mass Transfer*, 16, 1825- 1832.

[37] Cornini, G., Guidiq S.D., Lewis, RW., and Zienkiewiq O.C. (1974), 'Finite Element Solution of Non-linear Heat Conduction Problems with Reference to Phase Change," *International Journal for Numerical Methods in Engineering*, 8, 613-624.

[38] Morgan K., Lewis, RW. and Zienkiewicq OC (1978), 'An Improved Algorithm for Heat Conduction Problems with Phase Change', *International Journal for Numerical Methods in Engineering*, 12, 1191 -1195.

[39] Lemmon, E.C. (1981), 'Multidimensional Integral Phase Change Approximations for Finite Element Conduction Codes," *Numerical Methods in Heat Transfer*, Wiley, Chichester, 201-213.

[40] Pham, Q.T. (1986), 'The Use of Lumped Capacitance in the Finite-Element Solution of Heat Conduction Problems with Phase Change', *International Journal of Heat and Mass Transfer*, 29, 285-291.

[41] Esen M. and Durmus A. (1998), "Geometric design of solar-aided latent heat store depending on various parameters and phase change materials", *Solar Energy*, 62, 12-28.

[42] Rohsenow W. M., Hartnett J.P. and Ganic E. N. (1985) *Handbook of heat transfer fundementals*, 2nd edn, Rohsenow W. M. et al, (Eds). New York.